

Real-Time Optical Imaging of Primary Tumor Growth and Multiple Metastatic Events in a Pancreatic Cancer Orthotopic Model¹

Michael Bouvet, Jinwei Wang, Stephanie R. Nardin, Rounak Nassirpour, Meng Yang, Eugene Baranov, Ping Jiang, A. R. Moossa, and Robert M. Hoffman²

Department of Surgery, University of California San Diego, San Diego, California 92161 [M. B., S. R. N., R. N., A. R. M., R. M. H.], and AntiCancer, Inc., San Diego, California 92111 [J. W., M. Y., E. B., P. J., R. M. H.]

ABSTRACT

We report here whole-body optical imaging, in real time, of genetically fluorescent pancreatic tumors growing and metastasizing to multiple sites in live mice. The whole-body optical imaging system is external and noninvasive. Human pancreatic tumor cell lines, BxPC-3 and MiaPaCa-2, were engineered to stably express high-levels of the *Aequorea victoria* green fluorescent protein (GFP). The GFP-expressing pancreatic tumor cell lines were surgically orthotopically implanted as tissue fragments in the body of the pancreas of nude mice. Whole-body optical images visualized real-time primary tumor growth and formation of metastatic lesions that developed in the spleen, bowel, portal lymph nodes, omentum, and liver. Intravital images in the opened animal confirmed the identity of whole-body images. The whole-body images were used for real-time, quantitative measurement of tumor growth in each of these organs. Intravital imaging was used for quantification of growth of micrometastasis on the liver and stomach. Whole-body imaging was carried out with either a *trans*-illuminated epi-fluorescence microscope or a fluorescence light box, both with a thermoelectrically cooled color CCD camera. The simple, noninvasive, and highly selective imaging made possible by the strong GFP fluorescence allowed detailed simultaneous quantitative imaging of tumor growth and multiple metastasis formation of pancreatic cancer. The GFP imaging affords unprecedented continuous visual monitoring of malignant growth and spread within intact animals without the need for anesthesia, substrate injection, contrast agents, or restraint of animals required by other imaging methods. The GFP imaging technology presented in this report will facilitate studies of modulators of pancreatic cancer growth, including inhibition by potential chemotherapeutic agents.

INTRODUCTION

Pancreatic cancer is often a fatal disease with 5-year survival rates of only 1–4% (1). Reasons for low survival in this disease include aggressive tumor biology, high metastatic potential, and late presentation at the time of diagnosis (2). Clearly, new treatment modalities for this disease need to be explored if progress is to be made. To this end, we and others have developed orthotopic models of human pancreatic cancer in the nude mouse that simulate tumor growth, progression, and metastasis and allow for testing of novel treatment strategies (3–9).

Recently, we have improved these models by transforming the tumors with the *GFP*³ gene of the jellyfish *Aequorea victoria* to enable better detection of primary tumor growth and metastasis (10). Tracking of pancreatic cancer cells that stably express GFP *in vivo* is far more sensitive and rapid than the traditional cumbersome procedures of histopathological examination or immunohistochemistry. In other orthotopic GFP models such as lung cancer, prostate cancer, and

melanoma, GFP labeling markedly improves the ability to visualize metastases in fresh tissue (11–13).

A major advantage of GFP-expressing tumor cells is that imaging requires no preparative procedures, contrast agents, substrates, anesthesia, or light-tight boxes as do other imaging techniques (14). GFP imaging is thus uniquely suited for whole-body imaging of tumor growth and metastases in live animals (15–17). In the current study using stable, high GFP-expression pancreatic tumor cells (10), we demonstrate external, noninvasive, simultaneous real-time, whole-body as well as intravital fluorescence imaging of orthotopic pancreatic tumor growth and multiple metastasis in mouse models.

MATERIALS AND METHODS

Pancreatic Cancer Cell Lines. The BxPC-3 and MIA-PaCa-2 human pancreatic cancer cell lines were obtained from the American Type Culture Collection (Rockville, MD). The cells were maintained in DMEM supplemented with 10% FCS, 2 mM glutamine, 100 units/ml penicillin, 100 µg/ml of streptomycin, and 0.25 µg/ml of amphotericin B (Gibco-BRL, Life Technologies, Inc., Grand Island, NY). Both cell lines were incubated at 37°C in 5% CO₂.

GFP-Retroviral Transduction and Selection of High GFP-Expression MIA-PaCa-2 and BxPC-3 Pancreatic Cancer Cells. For *GFP* gene transduction, 20% confluent MIA-PaCa-2 or BxPC-3 cells were incubated with a 1:1 precipitated mixture of retroviral supernatants of the PT67 packaging cells and RPMI 1640 (Gibco-BRL, Life Technologies, Inc.) for 72 h. Fresh medium was replenished at this time. MIA-PaCa-2 or BxPC-3 cells were harvested by trypsin/EDTA 72 h after infection with the GFP retroviral supernatants and subcultured at a ratio of 1:15 into selective medium that contained 200 µg/ml of G418. The level of G418 was increased to 800 µg/ml stepwise. MIA-PaCa-2 and BxPC-3 clones expressing GFP (MIA-PaCa-2-GFP or BxPC-3-GFP) were isolated with cloning cylinders (Bell-Art Products, Pequannock, NJ) by trypsin/EDTA and were amplified and transferred by conventional culture methods. High GFP-expression clones were then isolated in the absence of G418 for >10 passages to select for stable expression of GFP.

Animals. Nude *nu/nu* mice were maintained in a barrier facility on HEPA-filtered racks. The animals were fed with autoclaved laboratory rodent diet (Teckland LM-485; Western Research Products, Orange, CA). All animal studies were conducted in accordance with the principles and procedures outlined in the NIH Guide for the Care and Use of Animals under assurance number A3873-1.

SOI. Pancreatic tumors, grown *s.c.* in nude mice, were harvested at the exponential growth phase and resected under aseptic conditions. Necrotic tissues were cut away, and the remaining healthy tumor tissues were cut with scissors and minced into approximately 3 × 3 × 3-mm pieces in HBSS containing 100 units/ml penicillin and 100 µg/ml streptomycin. Each piece was weighed and adjusted with scissors to be 50 mg. For orthotopic surgery, mice were anesthetized by injection of 0.02 ml of solution of 50% ketamine, 38% xylazine, and 12% acepromazine maleate. The abdomen was sterilized with alcohol. An incision was then made through the left upper abdominal pararectal line and peritoneum. The pancreas was carefully exposed, and three tumor pieces were transplanted on the middle of the pancreas with a 6-0 Dexon (Davis-Geck, Inc., Manati, Puerto-Rico) surgical suture. The pancreas was then returned to the peritoneal cavity, the abdominal wall, and the skin was closed with 6-0 Dexon sutures. Animals were kept in a sterile environment. All procedures of the operation described above were performed with a 7 × microscope (Olympus).

Received 10/31/01; accepted 1/4/02.

The costs of publication of this article were defrayed in part by the payment of page charges. This article must therefore be hereby marked *advertisement* in accordance with 18 U.S.C. Section 1734 solely to indicate this fact.

¹ Supported in part by National Cancer Institute Grant 1 R43 89779-01, the Department of Health Services, California Cancer Research Program 97-12013, and the UCSD Specialized Cancer Center support National Cancer Institute Grant P30 CA23100-18S1.

² To whom requests for reprints should be addressed, at AntiCancer, Inc., San Diego, CA 92111. Phone: (858) 654-2555; Fax: (858) 268-4175; E-mail: all@anticancer.com.

³ The abbreviations used are: GFP, green fluorescent protein; SOI, surgical orthotopic implantation.

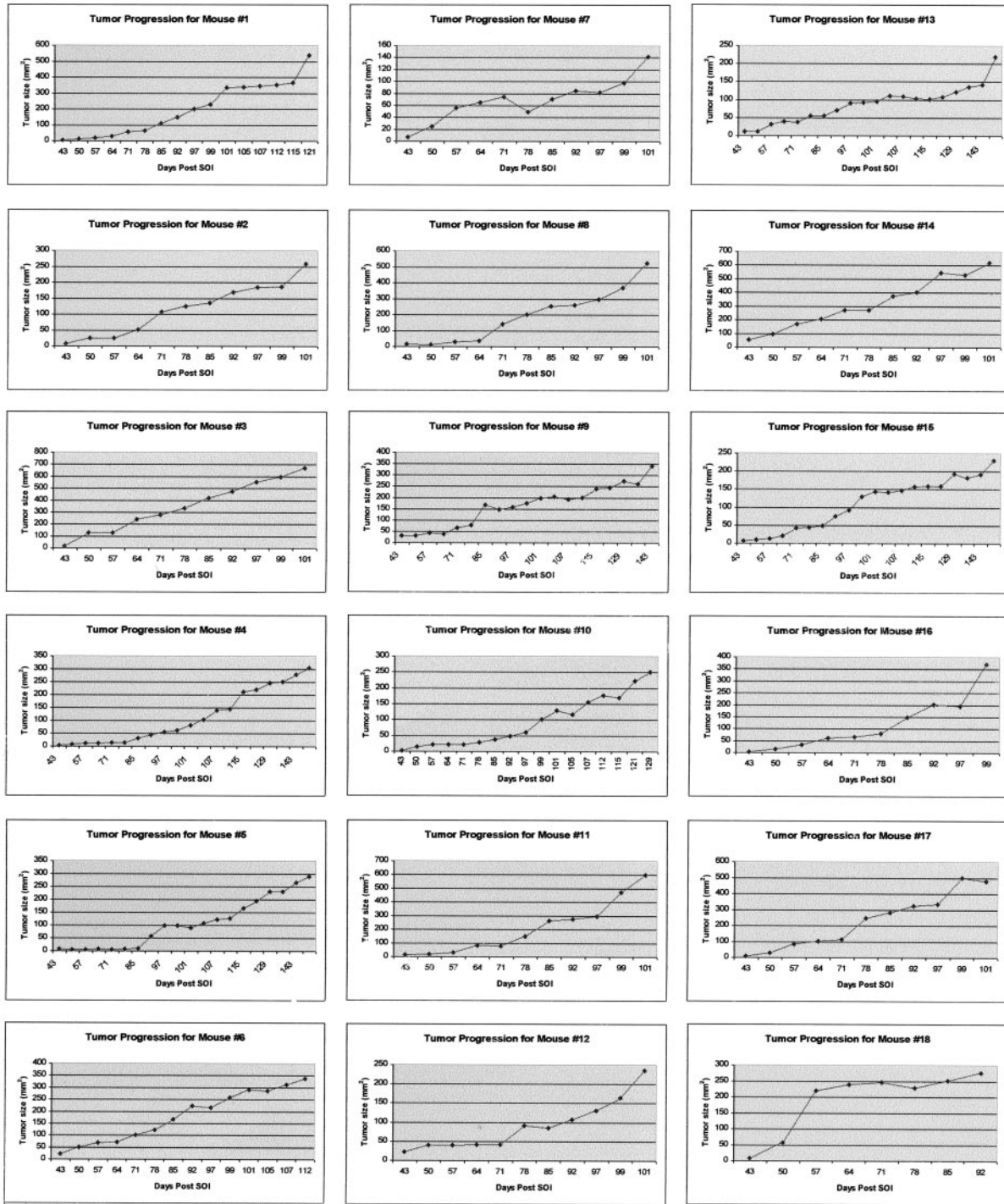


Fig. 1. Whole-body optical imaging of primary tumor growth in 18 orthotopically implanted pancreatic tumor-bearing mice. Consecutive external whole-body images of internally-growing BxPC-3 GFP tumors are demonstrated for 18 orthotopic mice. Although there were slight variations in tumor growth, a consistent increase in size was documented for each mouse by whole-body imaging without the need for laparotomy or any invasive procedure. See "Materials and Methods" for the GFP imaging procedure.

Portal Vein Injection. Six-week-old female B57Cl/6 mice were injected with 10^6 MiaPaCa-2-GFP cells in the portal vein. Cells were harvested by trypsinization and washed three times with cold serum-free medium and then injected in a total volume of 0.2 ml by using a 1-ml 27-gauge, latex-free syringe (Becton Dickinson, Franklin Lakes, NJ) within 30 min of harvesting.

Imaging. A Leica fluorescence stereo microscope model LZ12 (Leica Microsystems, Inc., Bannockburn, IL) equipped with a mercury 50W lamp power supply was used. Selective excitation of GFP was produced through a D425/60 band-pass filter and 470 DCXR dichroic mirror. Emitted fluorescence was collected through a long-pass filter GG475 (Chroma Technology, Brattle-

boro, VT) on a Hamamatsu C5810 3-chip cooled color CCD camera (Hamamatsu Photonics Systems, Bridgewater, NJ). Periodically, the tumor-bearing mice were also examined in a fluorescence light box illuminated by fiberoptic lighting at 440/20 nm with images collected with the Hamamatsu camera described above (Lighttools Research, Inc., Encinitas, CA). High resolution images of 1024×724 pixels were captured directly on an IBM PC or continuously through video output on a high-resolution Sony VCR model SLV-R1000 (Sony Corp., Tokyo Japan). Images were processed for contrast and brightness and analyzed with the use of Image Pro Plus 4.0 software (Media Cybernetics, Silver Springs, MD).

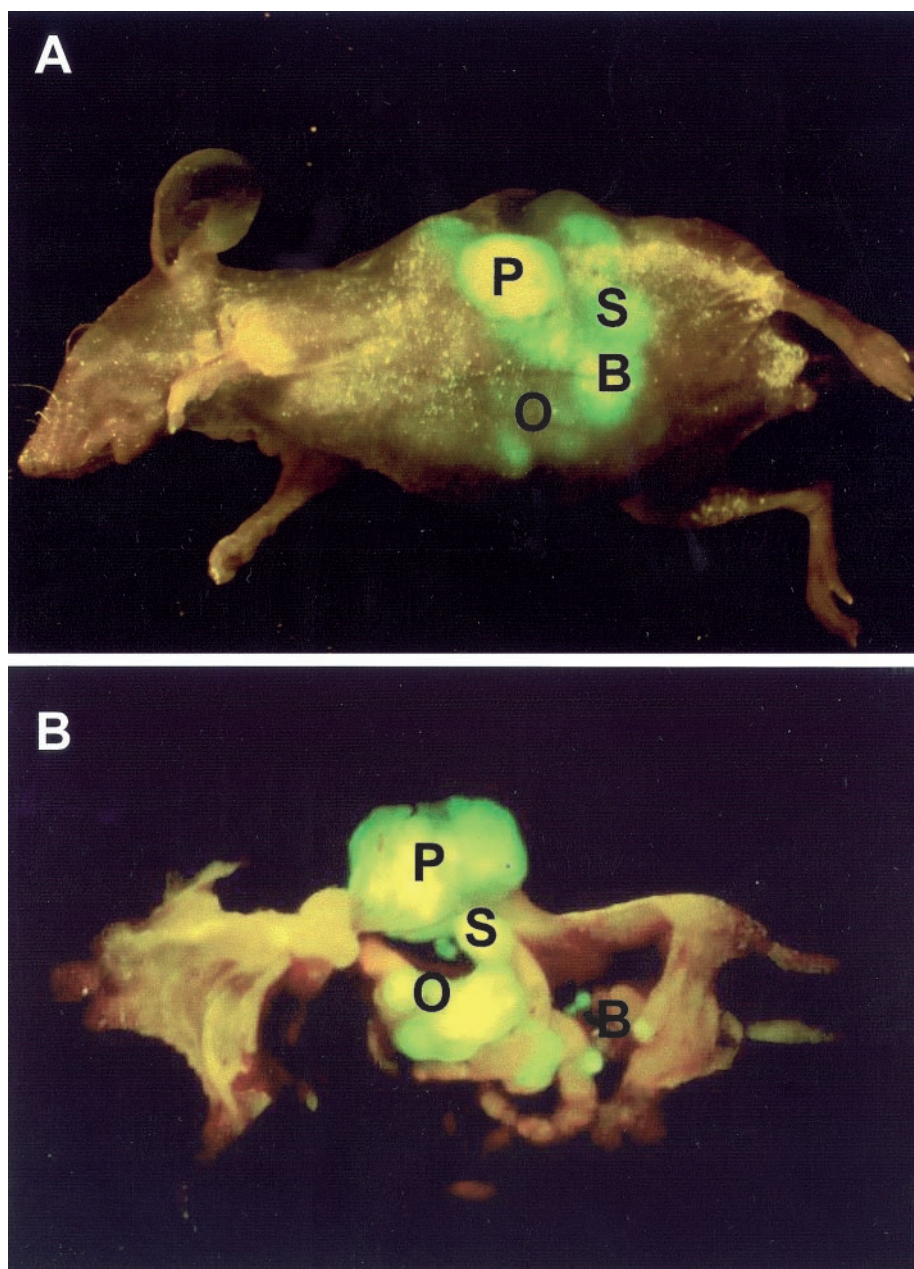


Fig. 2. External whole-body images of the BxPC-3-GFP primary tumor compared with internal images. See “Materials and Methods” for imaging equipment and procedures. *A*, fluorescent images of the primary pancreatic tumor (*P*), omental (*O*), bowel (*B*), and spleen (*S*) metastases. *B*, an image of the same mouse after laparotomy internally localized the external images of metastatic tumors.

The image detection sensitivity and resolution as a function of tumor size and depth of this technology have been described previously (18).

RESULTS

Isolation of Stable, High-Level Expression GFP Transductants of BxPC-3-GFP and MiaPaCa-2-GFP Cells. GFP- and neomycin-transduced BxPC-3 and MiaPaCa-2 cells were selected previously in multiple steps for growth in levels of Geneticin (G418) up to 800 $\mu\text{g/ml}$ and for high GFP expression (10). The selected BxPC-3-GFP and MiaPaCa-2-GFP cells have a strikingly bright GFP fluorescence that remains stable in the absence of selective agents after numerous passages (10).

Whole-Body Optical Imaging of Primary Tumor Growth in Orthotopically-Implanted Pancreatic Tumor-bearing Mice. Consecutive external whole-body images of internally growing BxPC-3-

GFP primary tumors are demonstrated for 18 mice (Fig. 1). Although there were slight variations in the rate of tumor growth, a consistent increase in size over ~ 100 days was documented for each mouse by whole-body imaging without the need for laparotomy or any invasive procedure.

Comparison of External Whole-Body and Direct Intravital Images of the BxPC-3-GFP Primary Tumor and Multiple Metastases. The primary pancreatic tumor as well as spleen, omental, and bowel metastases were simultaneously visualized by whole-body imaging through the skin of the nude mouse with GFP (Fig. 2A). An image of an opened mouse internally localizes the external images of primary and metastatic tumors (Fig. 2B).

Real-Time Simultaneous Whole-Body Imaging of BxPC-3-GFP Tumor and Multiple Metastatic Growths. Consecutive whole-body simultaneous images of the primary BxPC-3-GFP pancreatic tumor, spleen, bowel, and omentum metastases are shown in Fig. 3A. These images were simultaneously obtained in a single animal on

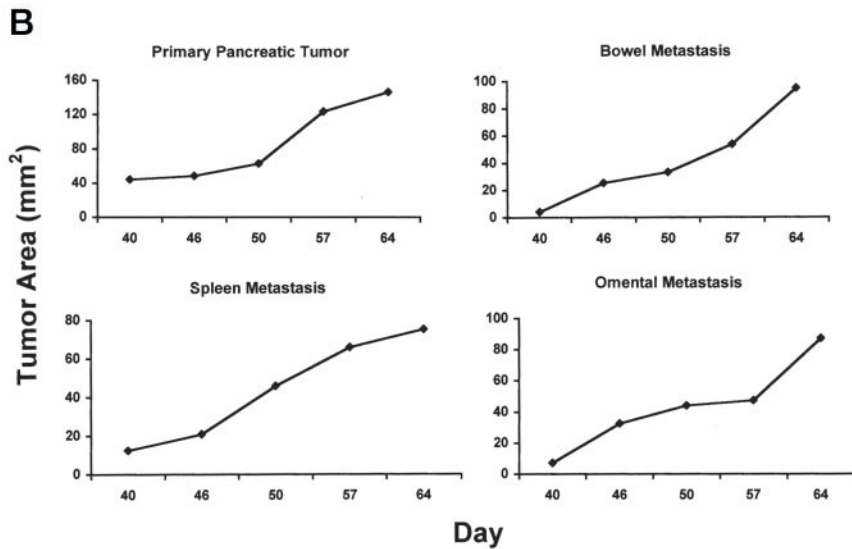
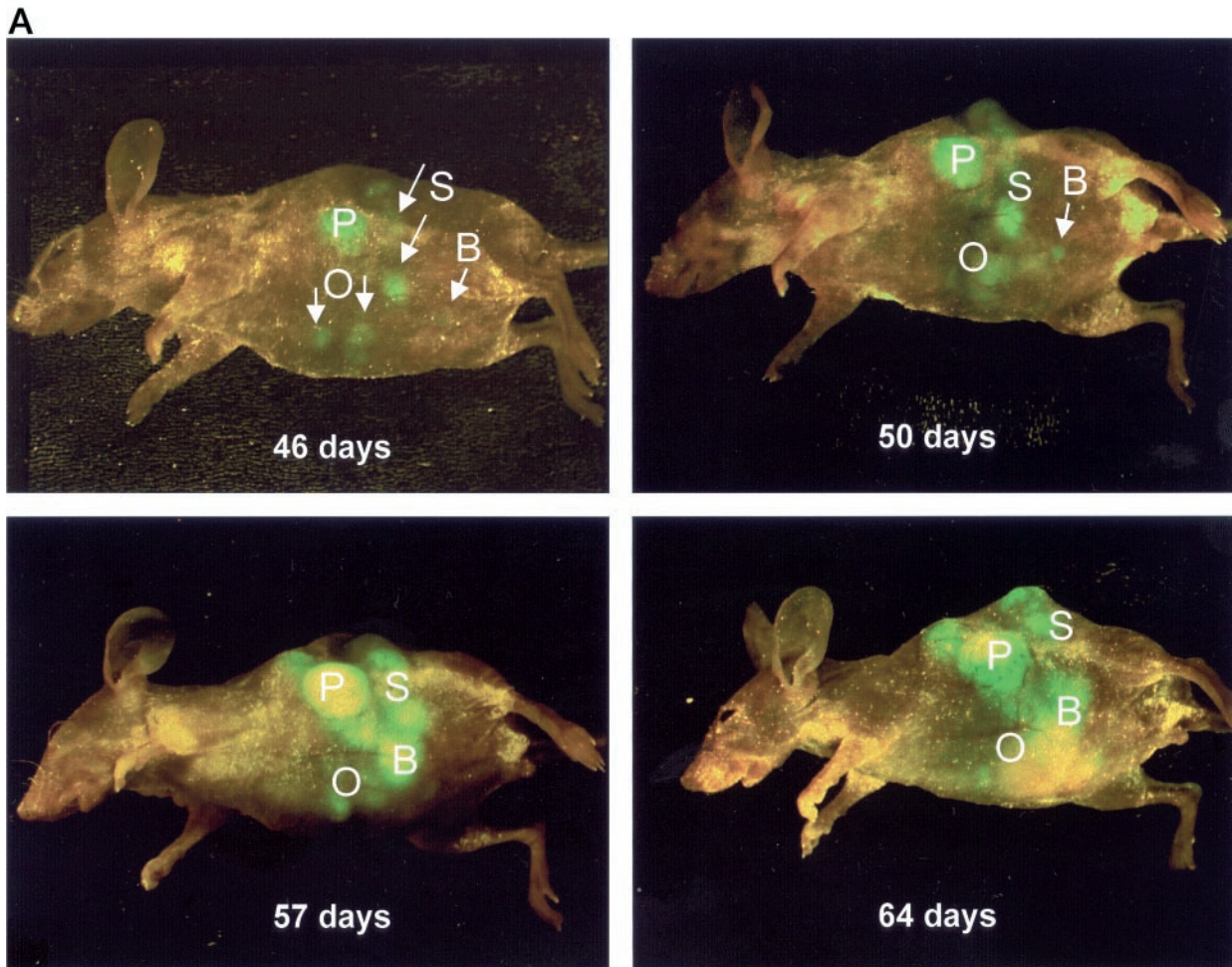


Fig. 3. A, consecutive external whole-body images of internally-growing BxPC-3-GFP tumors. A series of external fluorescence images of the BxPC-3-GFP pancreatic tumor in a single animal was obtained from days 46 to 64 after SOI of BxPC-3-GFP in a nude mouse. B, growth curves for primary pancreatic tumor (P), splenic metastasis (S), omental metastases (O), and bowel metastasis (B) as determined by whole-body imaging.

days 46, 50, 57, and 64 after SOI. In each of the sites, tumor growth and progression were quantified with image analysis. Growth curves (Fig. 3B) for the primary tumor and metastases at each of the above sites were constructed from the whole-body images. Thus, simultaneous metastases can be quantitated with whole-body imaging.

Comparison of Whole-Body and Intravital Images of Experimental Liver Metastasis of MiaPaCa-2-GFP. Metastatic lesions of MiaPaCa-2-GFP in the nude mouse liver were formed after portal vein injection. A clear external whole-body image of multiple metastatic lesions in the liver could be visualized through the

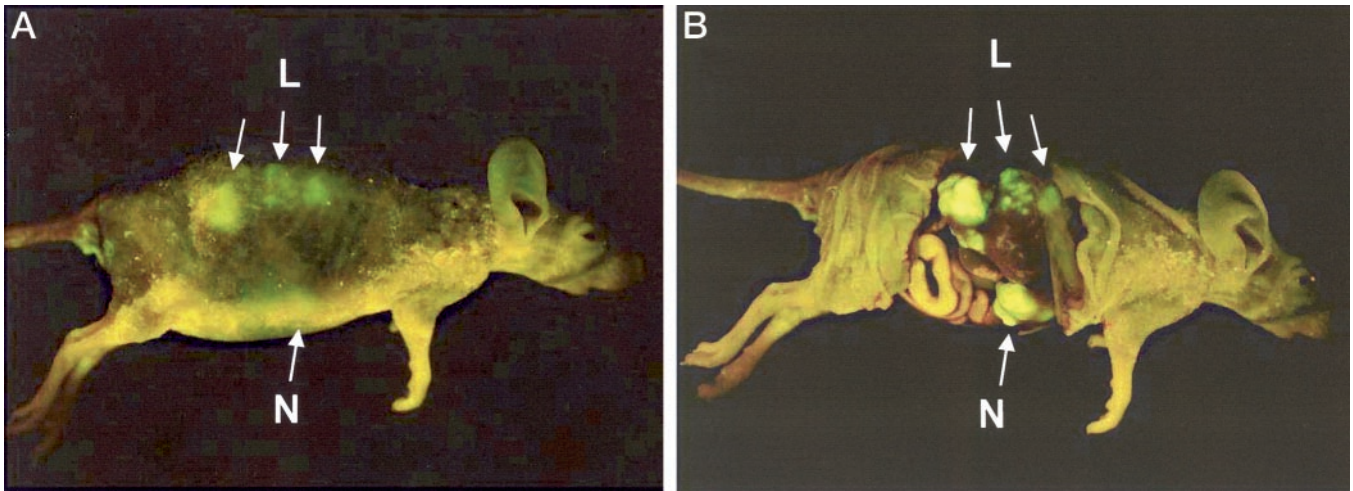


Fig. 4. *A*, external images of whole-body liver metastasis of MiaPaCa-2-GFP. Metastatic lesions of MiaPaCa-2-GFP in the nude mouse liver were formed after portal vein injection. A clear whole-body image of multiple metastatic lesions in the liver could be seen through the abdominal wall of the intact mouse. *B*, the whole-body image was comparable with the intravital image acquired from the exposed liver. *L*, liver metastases; *N*, nodal metastases.

abdominal wall of the intact mouse (Fig. 4A). Tumors were visualized throughout the multiple lobes of the liver. The whole-body image was comparable with the intravital image acquired from the exposed liver (Fig. 4B).

Sequential Intravital Images of Omental Micrometastasis of BxPC-3-GFP. A series of internal intravital fluorescence images of an omental micrometastasis from a BxPC-3-GFP pancreatic tumor in a single animal was obtained from days 36 to 70 after SOI of

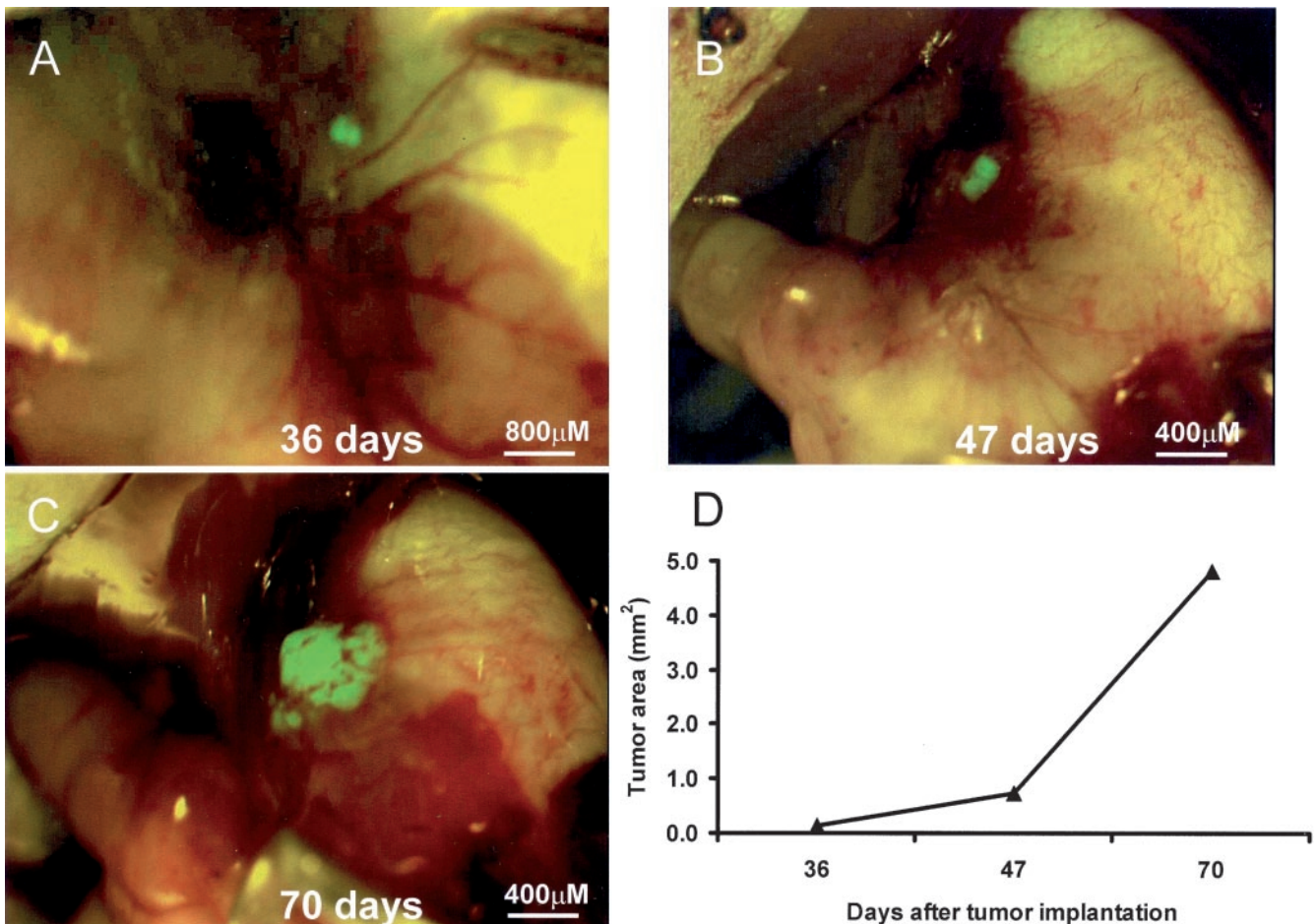


Fig. 5. Sequential intravital images of omental micrometastasis of BxPC-3-GFP. A series of internal fluorescence images of an omental micrometastasis from a BxPC-3-GFP pancreatic tumor in a single animal was obtained from days 36 to 70 after SOI of BxPC-3-GFP in a nude mouse during a laparotomy procedure (A–C). See “Materials and Methods” for details. As determined by internal imaging, the size of the metastatic lesion grew progressively with time (D). The area of the external image was 0.12 mm² at day 36, 0.74 mm² at day 47, and 4.8 mm² at day 70.

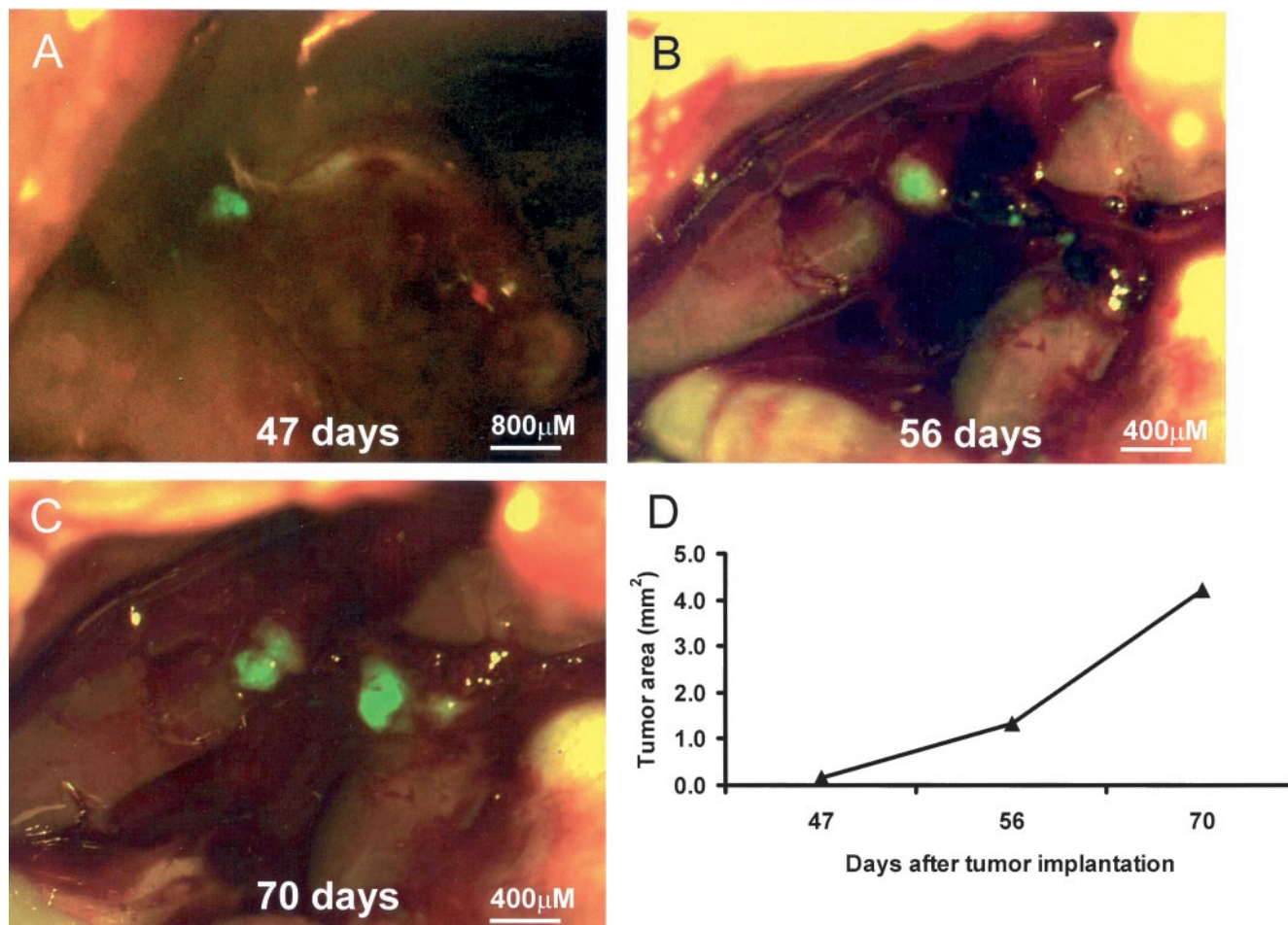


Fig. 6. Sequential intravital images of liver micrometastasis of BxPC-3-GFP. Internal images of liver metastases after SOI of BxPC-3-GFP tumor in nude mice were obtained during a laparotomy procedure (A–C). See “Materials and Methods.” The area of the metastatic lesion was 0.14 mm² at day 47, 1.33 mm² at day 56, and 4.22 mm² at day 70 (D).

BxPC-3-GFP in a nude mouse. The images were acquired during a laparotomy procedure. As determined by intravital imaging, the size of the metastatic lesion grew progressively with time (Fig. 5). The area of the external image was 0.12 mm² at day 36, 0.74 mm² at day 47, and 4.8 mm² at day 70.

Sequential Intravital Images of Liver Micrometastasis of BxPC-3-GFP. Fig. 6 show a series of intravital fluorescence images of liver micrometastases after SOI of BxPC-3-GFP in nude mice. The area of the metastatic lesion was 0.14 mm² at day 47, 1.33 mm² at day 56, and 4.22 mm² at day 70.

DISCUSSION

In this report, we demonstrate an orthotopic model of metastatic pancreatic cancer where primary and site-specific metastatic growth can be readily imaged by GFP fluorescence in real time. The whole-body imaging of primary pancreatic tumors (Fig. 1) correlated with the more established method of tumor weight measurement. The whole-body images correlate with direct intravital images (Figs. 2 and 4). The whole-body imaging data can be quantitated (Fig. 3), thereby eliminating cumbersome, tedious dissection of the primary tumor and its metastases. Most importantly, primary and site-specific metastatic tumor growth can be simultaneously visualized and quantified in real time in the same mouse by whole-body imaging. GFP-expressing pancreatic tumors enabled the intravital imaging of micrometastasis, which were followed over time in the liver and spleen by rapid laparotomy and image acquisition. This could be repeated for at least three time points (Figs. 5 and 6).

The GFP-based fluorescence optical tumor imaging system presents many powerful and unique features. GFP expression in the tumor cells is stable over indefinite time periods, allowing the quantitative imaging of tumor growth and metastasis formation. Only the tumors and metastases contain the heritable *GFP* gene and are therefore selectively imaged with very high intrinsic contrast to other tissues. The very bright GFP fluorescence enables internal tumors and metastases to be externally observed in critical organs, such as the pancreas, spleen, and liver. No contrast agents, substrates, radioactive materials, other compounds, anesthesia, or treatment need be administered to the animals; only blue light illumination is necessary.

The GFP-expressing pancreatic tumor model should be useful for the evaluation of novel treatment strategies for pancreatic cancer including neoadjuvant chemotherapy or gene therapy (19, 20). Such strategies are needed to combat this highly lethal tumor that is seldom curable. In addition, early detection of pancreatic cancer can be evaluated in this model by the measurement of serum tumor markers (21). Finally, a greater understanding of the aggressive growth and metastatic potential of pancreatic cancer will be facilitated by the use of GFP-expressing tumor cells.

REFERENCES

1. Bouvet, M., Gamagami, R. A., Gilpin, E. A., Romeo, O., Sasson, A., Easter, D. W., and Moossa, A. R. Factors influencing survival after resection for periampullary neoplasms. *Am. J. Surg.*, 180: 13–17, 2000.
2. Bouvet, M., Binmoeller, K. F., and Moossa, A. R. Diagnosis of adenocarcinoma of the pancreas. In: J. L. Cameron (ed.) *American Cancer Society Atlas of Clinical Oncology*, pp. 67–86: Pancreatic Cancer. Hamilton, Ontario, Canada: BC Decker, 2001.

3. Marincola, F. M., Drucker, B. J., Siao, D. Y., Hough, K. L., and Holder, W. D., Jr. The nude mouse as a model for the study of human pancreatic cancer. *J. Surg. Res.*, *47*: 520–529, 1989.
4. Bruns, C. J., Harbison, M. T., Kuniyasu, H., Eue, I., and Fidler, I. J. *In vivo* selection and characterization of metastatic variants from human pancreatic adenocarcinoma by using orthotopic implantation in nude mice. *Neoplasia*, *1*: 50–62, 1999.
5. Vezeridis, M. P., Doremus, C. M., Tibbetts, L. M., Tzanakakis, G., and Jackson, B. T. Invasion and metastasis following orthotopic transplantation of human pancreatic cancer in the nude mouse. *J. Surg. Oncol.*, *40*: 261–265, 1989.
6. Fu, X., Guadagni, F., and Hoffman, R. M. A metastatic nude-mouse model of human pancreatic cancer constructed orthotopically with histologically intact patient specimens. *Proc. Natl. Acad. Sci. USA*, *89*: 5645–5649, 1992.
7. An, Z., Wang, X., Kubota, T., Moossa, A. R., and Hoffman, R. M. A clinical nude mouse metastatic model for highly malignant human pancreatic cancer. *Anticancer Res.*, *16*: 627–631, 1996.
8. Furukawa, T., Kubota, T., Watanabe, M., Kitajima, M., and Hoffman, R. M. A novel patient-like treatment model of human pancreatic cancer constructed using orthotopic transplantation of histologically intact human tumor tissue in nude mice. *Cancer Res.*, *53*: 3070–3072, 1993.
9. Tomikawa, M., Kubota, T., Matsuzaki, S. W., Takahashi, S., Kitajima, M., Moossa, A. R., and Hoffman, R. M. Mitomycin C and cisplatin increase survival in a human pancreatic cancer metastatic model. *Anticancer Res.*, *17*: 3623–3625, 1997.
10. Bouvet, M., Yang, M., Nardin, S., Wang, X., Jiang, P., Baranov, E., Moossa, A., and Hoffman, R. Chronologically-specific metastatic targeting of human pancreatic tumors in orthotopic models. *Clin. Exp. Metastasis*, *18*: 213–218, 2000.
11. Yang, M., Jiang, P., An, Z., Baranov, E., Li, L., Hasegawa, S., Al-Tuwaijri, M., Chishima, T., Shimada, H., Moossa, A. R., and Hoffman, R. M. Genetically fluorescent melanoma bone and organ metastasis models. *Clin. Cancer Res.*, *5*: 3549–3559, 1999.
12. Yang, M., Jiang, P., Sun, F. X., Hasegawa, S., Baranov, E., Chishima, T., Shimada, H., Moossa, A. R., and Hoffman, R. M. A fluorescent orthotopic bone metastasis model of human prostate cancer. *Cancer Res.*, *59*: 781–786, 1999.
13. Chishima, T., Miyagi, Y., Wang, X., Baranov, E., Tan, Y., Shimada, H., Moossa, A. R., and Hoffman, R. M. Metastatic patterns of lung cancer visualized live and in process by green fluorescence protein expression. *Clin. Exp. Metastasis*, *15*: 547–552, 1997.
14. Budinger, T. F., Benaron, D. A., and Koretsky, A. P. Imaging transgenic animals. *Annu. Rev. Biomed. Eng.*, *01*: 611–648, 1999.
15. Flotte, T. R., Beck, S. E., Chesnut, K., Potter, M., Poirier, A., and Zolotukhin, S. A fluorescence video-endoscopy technique for detection of gene transfer and expression. *Gene Ther.*, *5*: 166–173, 1998.
16. Fu, X. Y., Besterman, J. M., Monosov, A., and Hoffman, R. M. Models of human metastatic colon cancer in nude mice orthotopically constructed by using histologically intact patient specimens. *Proc. Natl. Acad. Sci. USA*, *88*: 9345–9349, 1991.
17. Sun, F. X., Sasson, A. R., Jiang, P., An, Z., Gamagami, R., Li, L., Moossa, A. R., and Hoffman, R. M. An ultra-metastatic model of human colon cancer in nude mice. *Clin. Exp. Metastasis*, *17*: 41–48, 1999.
18. Yang, M., Baranov, E., Jiang, P., Sun, F.-X., Li, X.-M., Li, L., Hasegawa, S., Bouvet, M., Al-Tuwaijri, M., Chishima, T., Shimada, H., Moossa, A. R., Penman, S., and Hoffman, R. M. Whole-body optical imaging of green fluorescent protein-expressing tumors and metastases. *Proc. Natl. Acad. Sci. USA*, *97*: 1206–1211, 2000.
19. Bouvet, M., Bold, R. J., Lee, J., Evans, D. B., Abbruzzese, J. L., Chiao, P. J., McConkey, D. J., Chandra, J., Chada, S., Fang, B., and Roth, J. A. Adenovirus-mediated wild-type *p53* tumor suppressor gene therapy induces apoptosis and suppresses growth of human pancreatic cancer. *Ann. Surg. Oncol.*, *5*: 681–688, 1998.
20. Lee, N.C., Bouvet, M., Nardin, S., Jiang, P., Baranov, E., Rashidi, B., Yang, M., Wang, X., Moossa, A. R., and Hoffman, R. M. Antimetastatic efficacy of adjuvant gemcitabine in a cancer pancreatic cancer orthotopic model. *Clin. Exp. Metastasis*, *18*: 379–384, 2000.
21. Bouvet, M., Nardin, S. R., Burton, D. W., Lee, N. C., Yang, M., Wang, X., Baranov, E., Behling, C., Moossa, A. R., Hoffman, R. M., and Deftos, L. J. Parathyroid hormone-related protein acts as a tumor marker in an orthotopic model of pancreatic adenocarcinoma. *Pancreas*, in press, 2002.